5. MECHANISM OF ACTIVE BOUNDARY LAYER CONTROL

It is important to understand the mechanism of active separation control in the actual use of vortex generator jets. In this chapter, in order to investigate the mechanism for suppressing flow separation, experiments are described which make a comparison between the two roles of steady and pulsed jets in generating longitudinal vortices. Mean velocity profiles, the downstream development of longitudinal vortices, secondary flow vectors, and contours of streamwise vorticity will be presented for the purpose of understanding the mechanism for preventing flow separation.

5.1 Experimental Method

A schematic diagram of the wind tunnel used is shown in Fig. 3.1. In this experiment, two freestream velocities U_0=6.5 and 11.1 m/s were chosen. The test section was configured with a lower wall which had a divergence angle of 20 or 30 degrees. A detailed diagram of the test section is shown in Fig. 3.2. The magnitude of the jet flow rate was characterized by the jet-to-freestream velocity ratio *VR*. The vortex generator jet device is shown in Fig. 3.12. The pulse rate was allowed up to 23 Hz. The configuration of jets and the coordinate system used to describe the flowfield are shown in Fig. 3.3. Three jets 2 mm in diameter were placed at the upstream of the divergent lower wall and their orifices were configured on the right-hand side of the lower wall in the test section (viewed from upstream). The jets in this study were skewed at 90 degrees to the freestream direction and pitched at 45

degrees to the lower wall.

Velocity profiles in the test section were obtained using an X-array hot wire probe. The hot wire probe was supported by a three-axis computer-controlled traverse unit. Streamwise velocity profiles were measured at Z=110 mm to avoid the effect of jet orifices. The downstream locations were chosen at X=40, 70, 110 mm. The velocity measurements in a Y-Z plane were carried out at equal spaces of 5 mm, in the X and Y directions.

5.2 Results and Discussion

5.2.1 Waveform of Pulsed Jets

Figure 5.1 shows the waveform of the pulsed jets in this study. The pulsed jet generator has a tendency to broaden the peak region of the waveform for both cases of increasing the jet flow rate (or equally increasing jet speed) and the lowering of a frequency. The feature of the frequency-lowering case results from the increased passage time of the secondary air due to decreased rotor speed.

5.2.2 Flow Visualization Results

The surface tuft method was used as a diagnostic technique to observe the effect of vortex generator jets on separated flow. Tufts were put on the lower wall of the test section at Z=125 and 140 mm. Figure 5.2 shows the surface flow in the divergent portion of the test section and the air flows from left to right. Figures 5.2(a), 5.2(b), and 5.2(c) indicate an unforced (non-issuing jets) case, the pulsed jet case, and the steady jet case, respectively. It is seen that steady or pulsed vortex generator jets can delay flow separation in comparison with the

unforced case.

5.2.3 Streamwise Velocity Measurements

Figures 5.3 and 5.4 show the streamwise velocity profiles in the test section. The data are presented for a lower wall divergence of 20 degrees. The profiles for the unforced case in these figures indicate a boundary layer separation in the divergent portion of the test section. For U_0=6.5 and 11.1 m/s, pulsed jets lead to a greater velocity increase in the near-wall region at the measurement stations of the divergent portion in comparison with the unforced case. Figure 5.3 shows that the effective near-wall velocity increase is achieved by increasing the jet flow rate. This result coincides with the conclusion for steady jets by Compton and Johnston [18] which states that a strong vortex could be produced by increasing the jet flow rate in the same freestream speed.

On the other hand, the velocity profiles for the case of U_0=11.1 m/s are similar for the two different *VR* of the pulsed jet case (see Fig. 5.4). In this study, we define positive vortices in a *Y-Z* plane for clockwise rotating ones when we view from upstream. Figure 5.5 shows a comparison between the downstream decays of the maximum positive vorticity and the minimum negative vorticity of longitudinal vortices. The positive vorticity produced by the interaction between the jets and the freestream becomes strong with increasing freestream velocity at a fixed *VR*. In other words, the case of U_0=11.1 m/s generates longitudinal vortices that are strong enough to achieve the near-wall velocity increase.

Two cases of jet pulse frequency, f_p=10 and 20 Hz, were investigated. The shapes of peaks in the original waveform of pulsed jets broaden with respect to the time axis and also the jet flow rate per pulse is increased by lowering the pulse frequency. In contrast, increasing the pulse frequency leads to an increase in the number of

peaks in the original waveform in a time interval. However, the profiles for f_p=20 Hz (see Fig. 5.6) show that the near-wall velocity is increased in comparison with those for f_p=10 Hz. In the present experiment, it is thus concluded that increasing the pulse frequency is more effective in the control of flow separation in comparison with broadening the shapes of peaks by lowering the pulse frequency.

The velocity profile for steady jets (see Fig. 5.4(a)) shows a velocity defect near the outer edge of the boundary layer of the unforced case, while the pulsed jets have the ability to thin the boundary layer thickness. Figure 5.7 shows streamwise flow vectors at X=40, 70, 110 mm. For the case of pulsed jets, downward flow vectors exist in the measurement region. On the other hand, for the case of steady jets, upward flow vectors exist near the outer edge of the boundary layer. In the steady jet case, there is a velocity defect because downward flow does not exist near the outer edge of the boundary layer in contrast with the pulsed jet case (see Fig. 5.7).

The correlation of U and V with respect to the period of pulsed jets and the velocity measurements for the case of pulsed jets are shown in Fig. 5.8. For f_p=20 Hz and the sampling time of 30 ms of streamwise velocity, issuing jets coincides with the sampling at every interval of 150 ms. A streamwise velocity decrease is observed at that time. In other words, if the velocity is measured at the instant that the jets are blown, a streamwise velocity decrease is observed. It is hence supposed that steady jets have a tendency to increase the velocity in Y direction near the outer edge of the boundary layer and also to decrease the streamwise velocity there.

For the vortex generator jet method, an increase in the jet flow rate causes a near-wall velocity increase and makes effective the control of the separated flow for the same freestream speed. The increase in the jet flow rate corresponds to the broadening of the shape of the peaks of the pulsed jets. In order to avoid a velocity defect near the outer edge of the boundary layer, the pulsed jet method therefore is important.

5.2.4 Velocity Measurements in a Y-Z Plane

Figures 5.9 and 5.10 show the downstream development of longitudinal vortices for the case of pulsed jets. Secondary flow vectors at X=70, 110 mm are shown in Fig. 5.11. Figures 5.9 and 5.10 indicate that the longitudinal vortices persist near the lower wall in the downstream direction. No strong vortices exist apart from the lower wall. From Fig. 5.11 it is seen that the secondary flow toward the lower wall is induced by the effect of the longitudinal vortices in the near-wall region. The secondary flow of longitudinal vortices may transport the high momentum fluid of the freestream to the lower wall. The suppression of flow separation in a separated flowfield is accomplished by transporting the high momentum fluid of the freestream to the lower wall.

Figure 5.12 shows the downstream development of longitudinal vortices for the case of steady jets. A comparison between Fig. 5.9 or 5.10 and Fig. 5.11 makes clear that the downstream development of longitudinal vortices for the case of pulsed jets is quite different from that for the case of steady jets. Pulsed jets keep the vortices near the lower wall. Because pulsed jets enhance the mixing process between the jets and the freestream further than steady jets, the upward movement of longitudinal vortices is suppressed.

From Fig. 5.12 counter-rotating vortices (with a negative sign) on the upwash side of the longitudinal vortices at X=10 mm are seen to be produced. It is supposed that the counter-rotating vortices are induced by the longitudinal vortices moving away from the lower wall. Vortex pairs are then formed. Three pairs of positive and negative vortices align on the right-hand side of Fig. 5.12 corresponding to the three jets. The formation of vortex pairs is due to the steady jets which make ineffective the mixing process between the jets and the freestream. The suppression of mixing brings about the upward movement of vortices. The pairs of vortices continue to be lifted away from the lower wall in the downstream direction due to the velocity induced by each vortex pair itself. The vortices, except for the edge

vortices on both sides of this array, become weaker and disappear in the downstream direction. The secondary flow vectors at X=70, 110 mm are shown in Fig. 5.13. An upward secondary flow is produced near Z=110 mm. It is plausible that the upwash is induced by a vortex pair formed as a result of the production of a counter-rotating vortex of nearly equal strength (see Fig. 5.12).

For the case of steady jets, the minimum negative vorticity has a strength nearly equal to the maximum positive vorticity. On the other hand, for the case of pulsed jets, the maximum strength of positive vorticity increases with increasing freestream velocity, while that of negative vorticity is almost unchanged for various freestream velocities (see also Fig. 5.5). The suppression effect against the upward flow is achieved by keeping the longitudinal vortices near the lower wall. These vortices can effectively transport the high momentum fluid of the freestream to the lower wall.

Figure 5.14 shows the contours of the streamwise velocity. For the case of steady jets, the contours exhibit strong distortion near the outer edge of the boundary layer near Z=110 mm and therefore the boundary layer thickness increases. This is due to the upwash induced by a pair of vortices of nearly equal strength at the spanwise location (see Fig. 5.13). Even if the suppression effect against separation is achieved, with the steady jet case the upwash makes ineffective the secondary flow toward the lower wall in a narrow spanwise region. Moreover, the velocity defect near the outer edge of the boundary layer is brought about by the upwash and thereby the boundary layer thickness varies largely in the spanwise direction. This characteristic is also confirmed in Fig. 5.3 where the mean velocity for the steady jet case is much lower than that for the unforced case. It should be noted that the streamwise velocity measurements are carried out just at Z=110 mm where the upwash occurs (see Fig. 5.14(b)).

5.2.5 Application for Divergence Angle of 30

Degrees

Figure 5.15 shows the streamwise velocity profiles at X=110 mm in the case of a divergence angle of 30 degrees for the pulsed jet case. The profiles indicate that the near-wall velocity hardly increases. Figure 5.16 shows the downstream development of the longitudinal vortices produced by the interaction between the pulsed jets and the freestream. The longitudinal vortices begin to lift away from the lower wall at X=70 mm and exist far from the lower wall at X=110 mm. A counter-rotating vortex of nearly equal strength exists below the longitudinal vortex because it moves away from the lower wall. Accordingly, the secondary flow toward the lower wall cannot be produced, as seen in Fig. 5.17. Figure 5.18 indicates the flow situation at X=110 mm for U_0=11.1 m/s. It is seen that the behavior of longitudinal vortices for U_0=11.1 m/s is similar to that for U_0=6.5 m/s. The high momentum fluid of the freestream is not carried effectively toward the lower wall and as a result the near-wall velocity in the divergent portion of the test section does not increase.

5.3 Conclusions

From the present experimental study on the mechanism of active boundary layer control using longitudinal vortices, the following conclusions were drawn:

1. The suppression of flow separation is achieved by the secondary flow of longitudinal vortices, produced by the interaction between the jets and the freestream, which transports the high momentum fluid of the freestream toward the lower wall.

2. If a counter-rotating vortex is induced by the vortex which moves away from the lower wall, a pair of vortices is formed. An

upwash is induced by the pair of vortices and as a result the boundary layer thickness is strongly distorted. The thickness becomes inhomogeneous in the spanwise direction because the streamwise velocity decreases in the upwash region.

3. The increase in near-wall velocity in the divergent portion of the test section is achieved by adjusting the strength of longitudinal vortices which depends on the jet flow rate. Pulsed jets enhance the mixing process between the jets and the freestream further compared with steady jets. This keeps longitudinal vortices close to the lower wall and never produces any upwash.

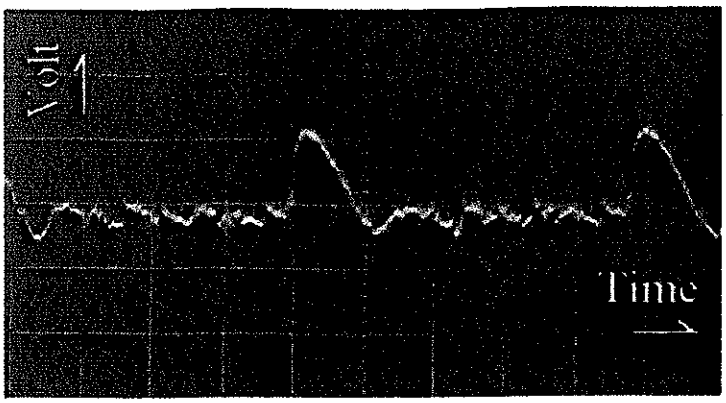

(a) f_p=20 Hz, Q_f=20 l/min (Time interval=10 ms)

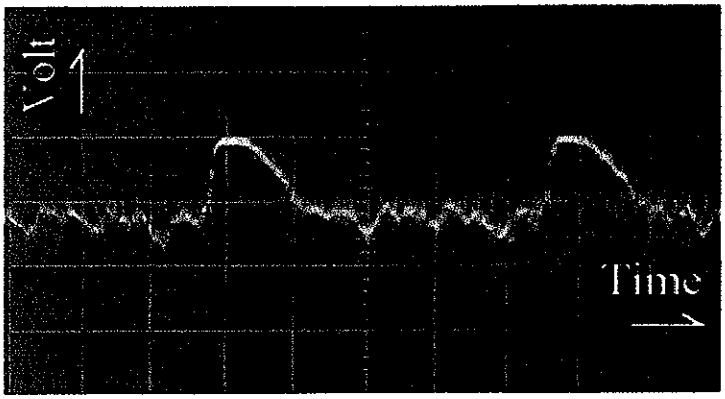

(b) f_p=20 Hz, Q_f=60 l/min (Time interval=10 ms)

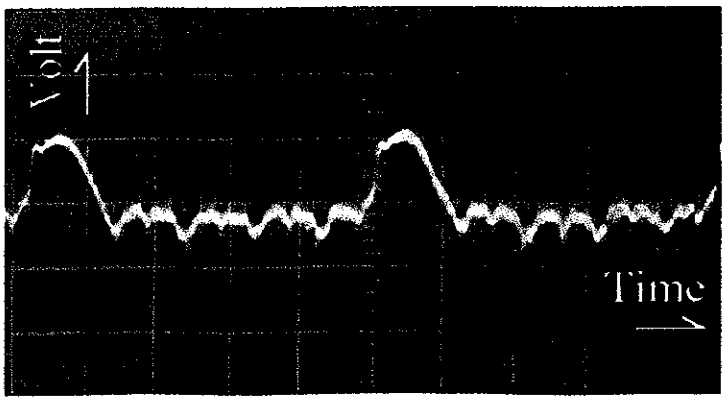

(c) f_p=10 Hz, Q_f=60 l/min (Time interval=20 ms)

Figure 5.1 Original waveform of pulsed jets.

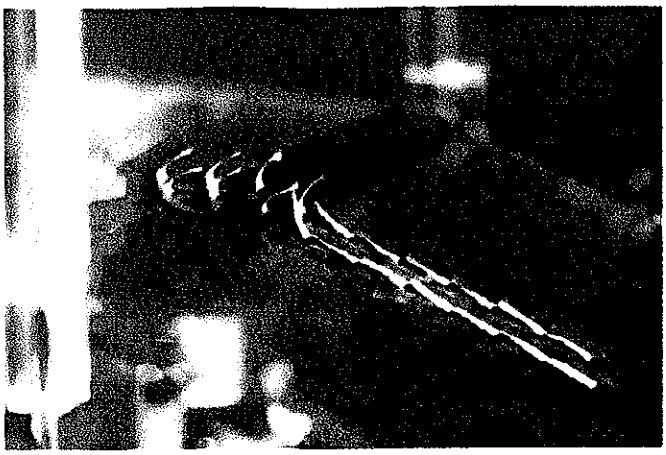

(a) Unforced

(b) VR=9.5, f_p=20 Hz

(c) VR=13

Figure 5.2 Surface flow in divergent portion of the test section (U_0=6.5 m/s).

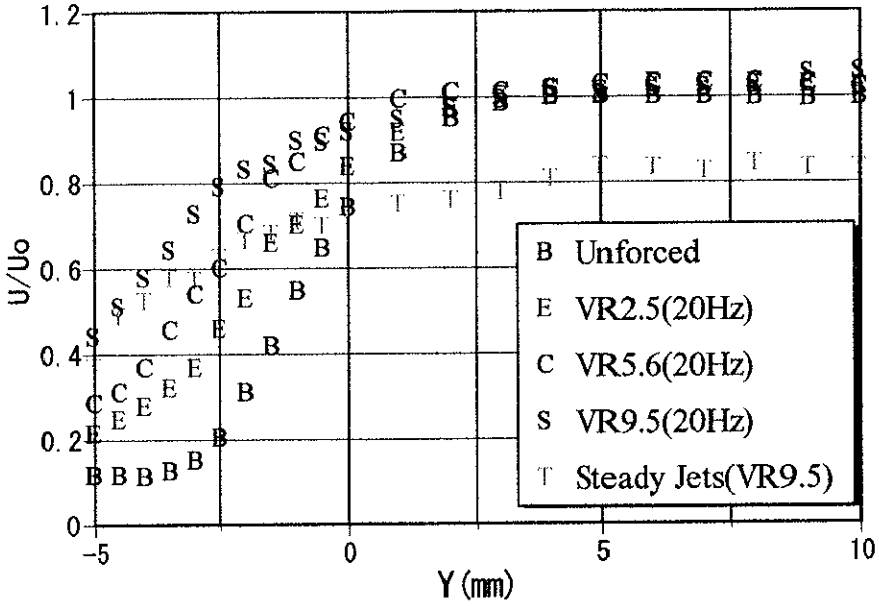

(a) X=70 mm

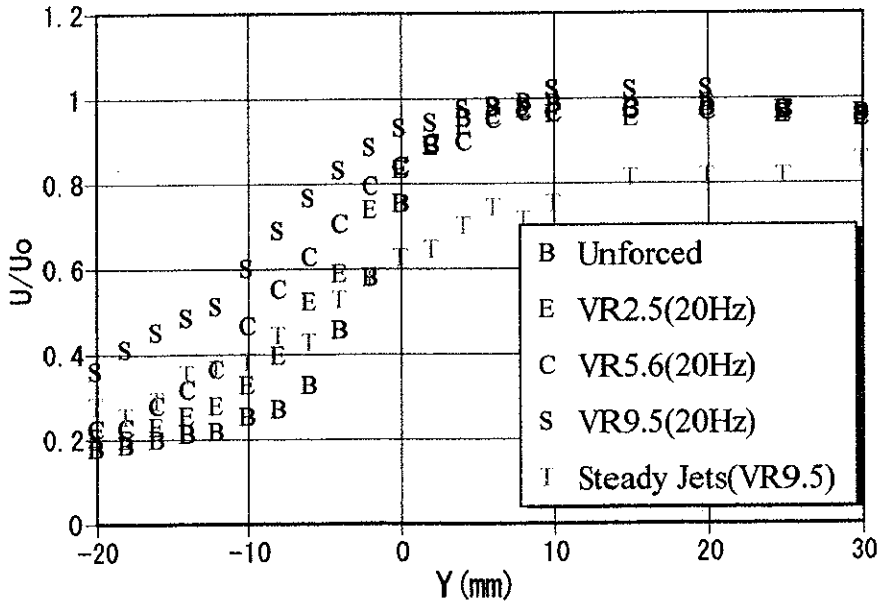

(b) X=110 mm

Figure 5.3 Streamwise velocity profiles (U_0=6.5 m/s,α =20 deg).

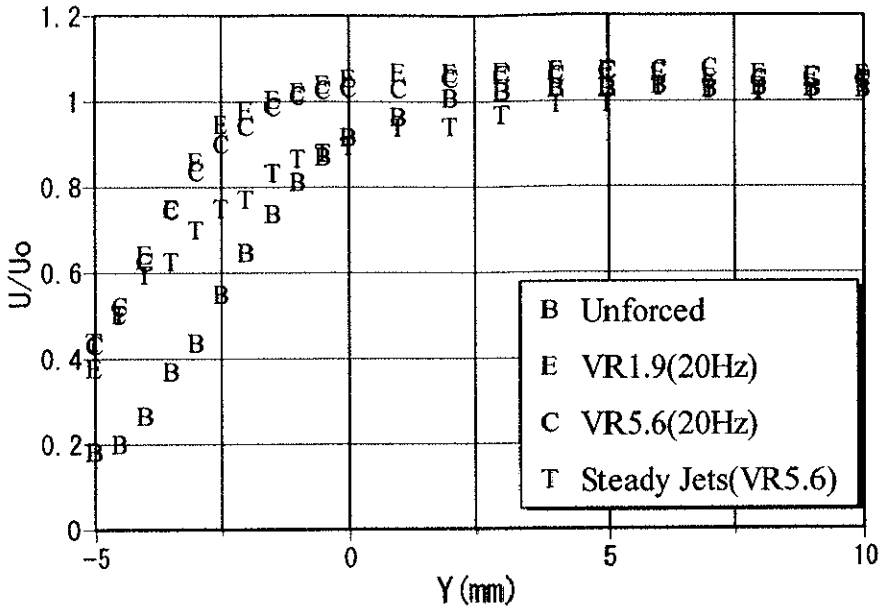

(a) X=70 mm

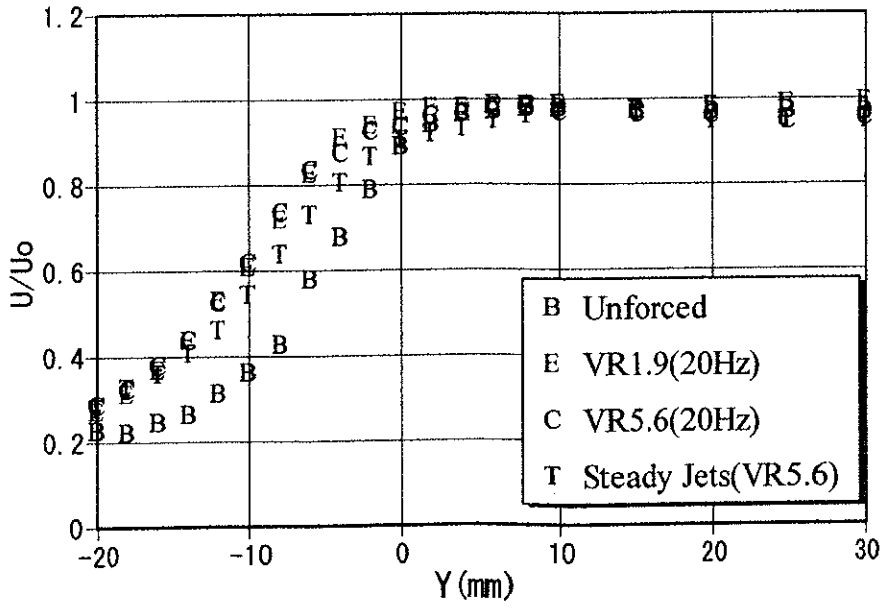

(b) X=110 mm

Figure 5.4 Streamwise velocity profiles (U_0=11.1 m/s, α=20 deg).

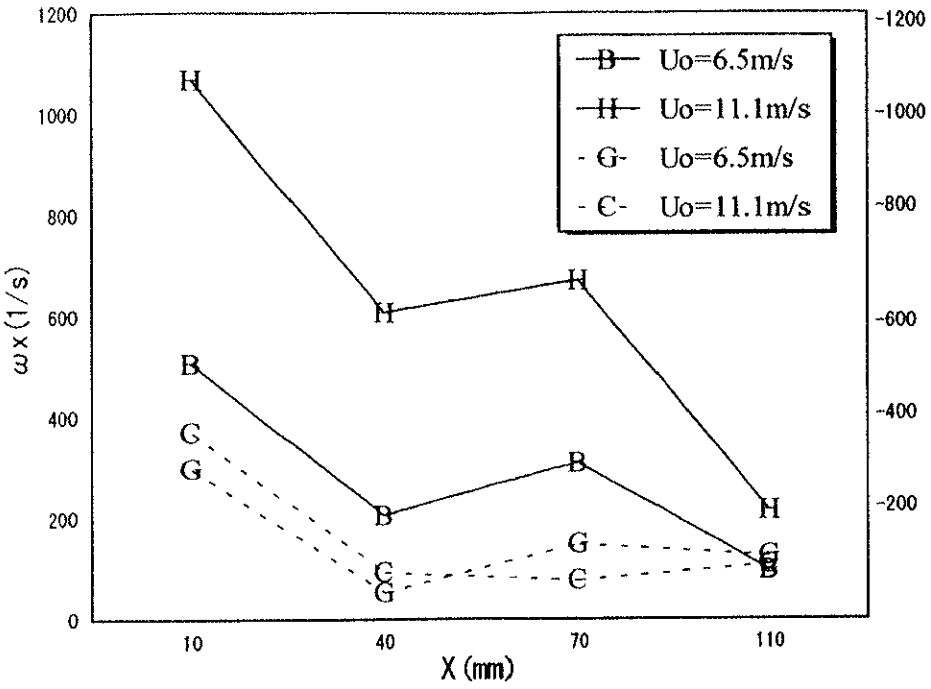

Figure 5.5 Comparison between the downstream decays of the maximum positive vorticity and the minimum negative vorticity. Open symbols denote negative vorticity (VR=5.6, f_p=20 Hz, α=20 deg).

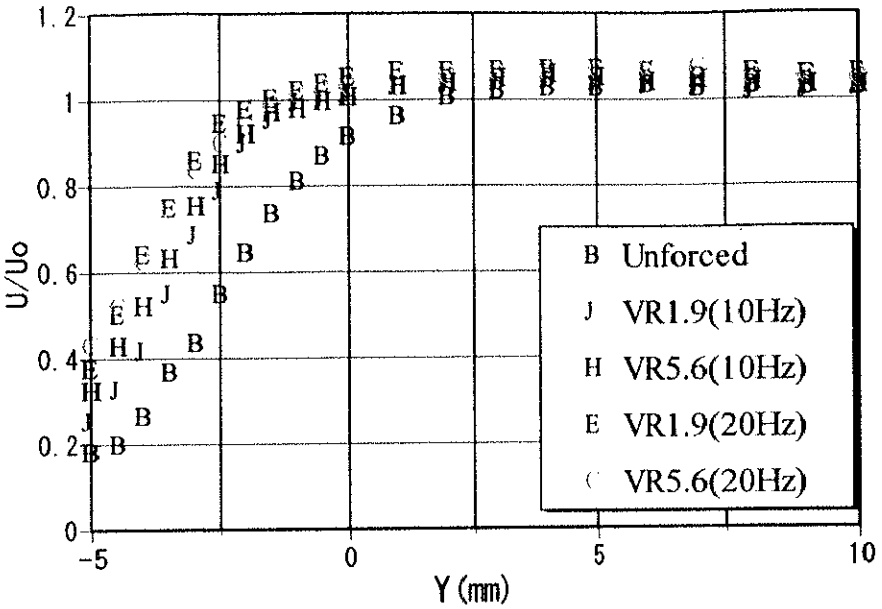

(a) X=70 mm

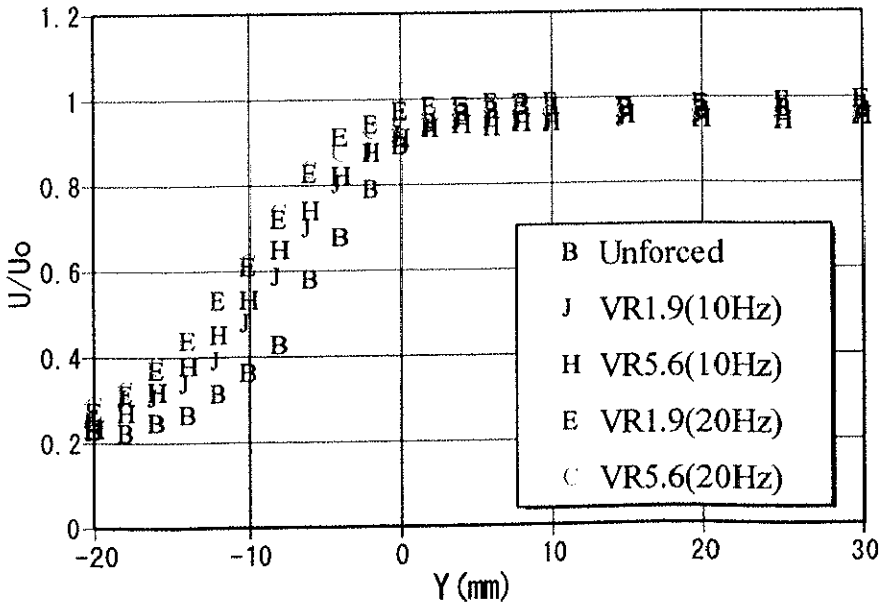

(b) X=110 mm

Figure 5.6 Streamwise velocity profiles for two cases of pulse frequency (U_0=11.1 m/s, α=20 deg).

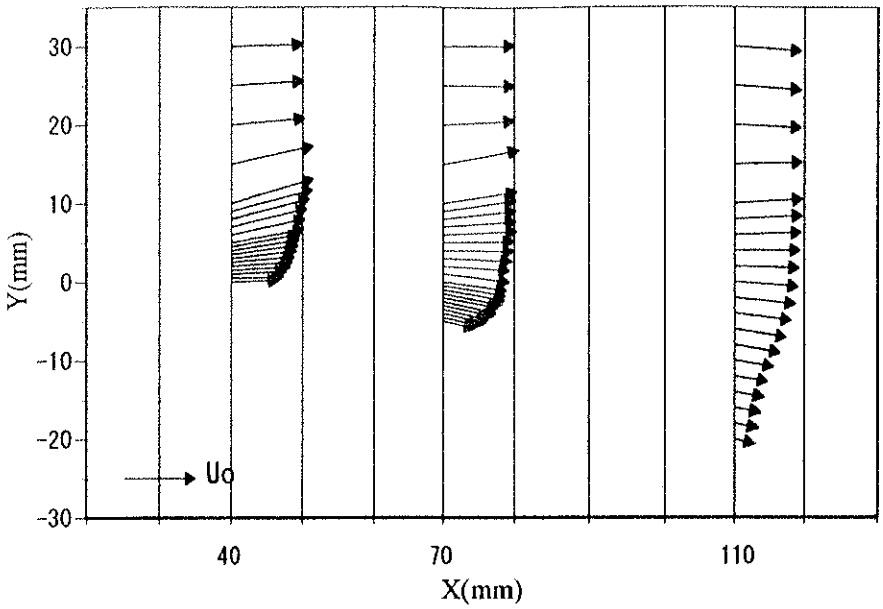

(a) Steady jets (VR=5.6)

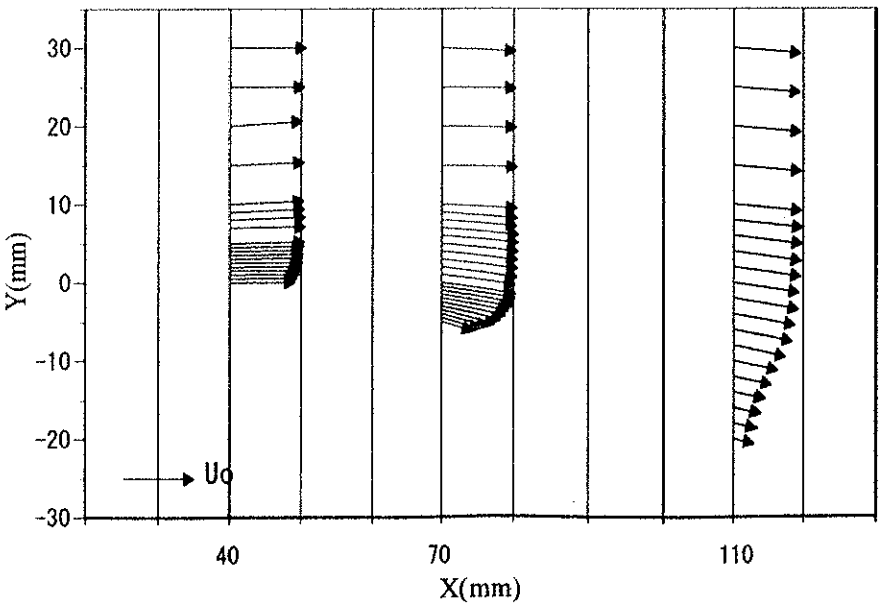

(b) Pulsed jets (VR=5.6, f_p=20 Hz)

Figure 5.7 Streamwise flow vectors (U_0=11.1 m/s, α=20 deg).

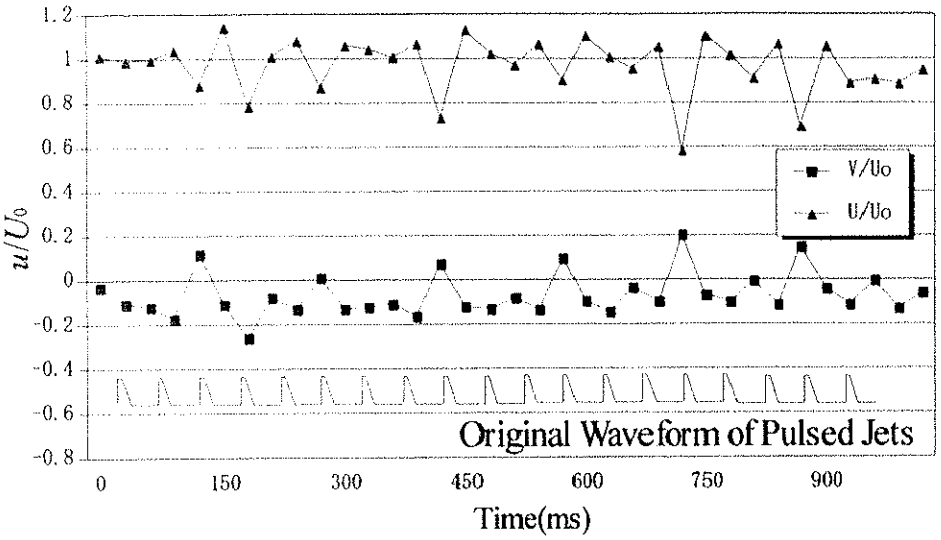

(a) U_0=6.5 m/s, VR=5.6, f_p=20 Hz

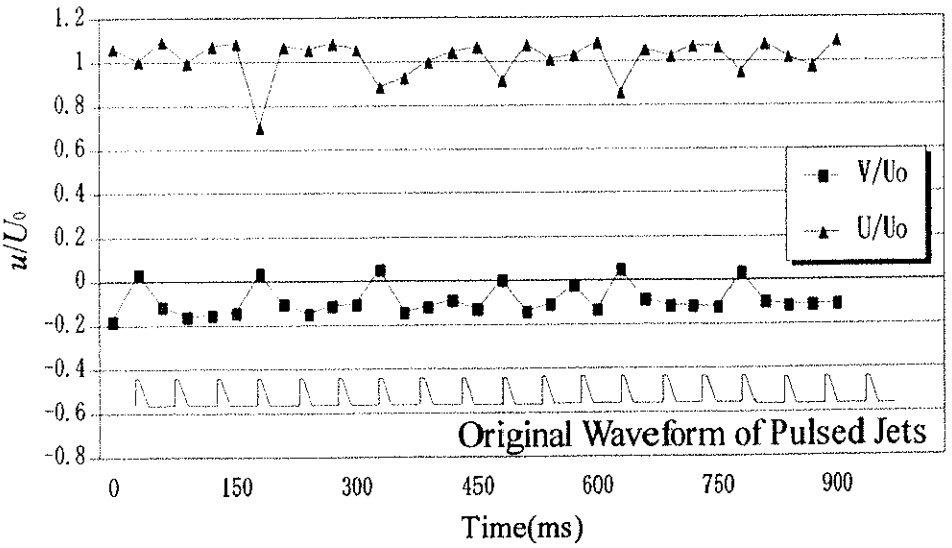

(b) U_0=11.1 m/s, VR=1.9, f_p=20 Hz

Figure 5.8 Sampling interval of streamwise velocity, compared to original waveform of pulsed jets at X=70 mm, Y=6 mm (α =20 deg).

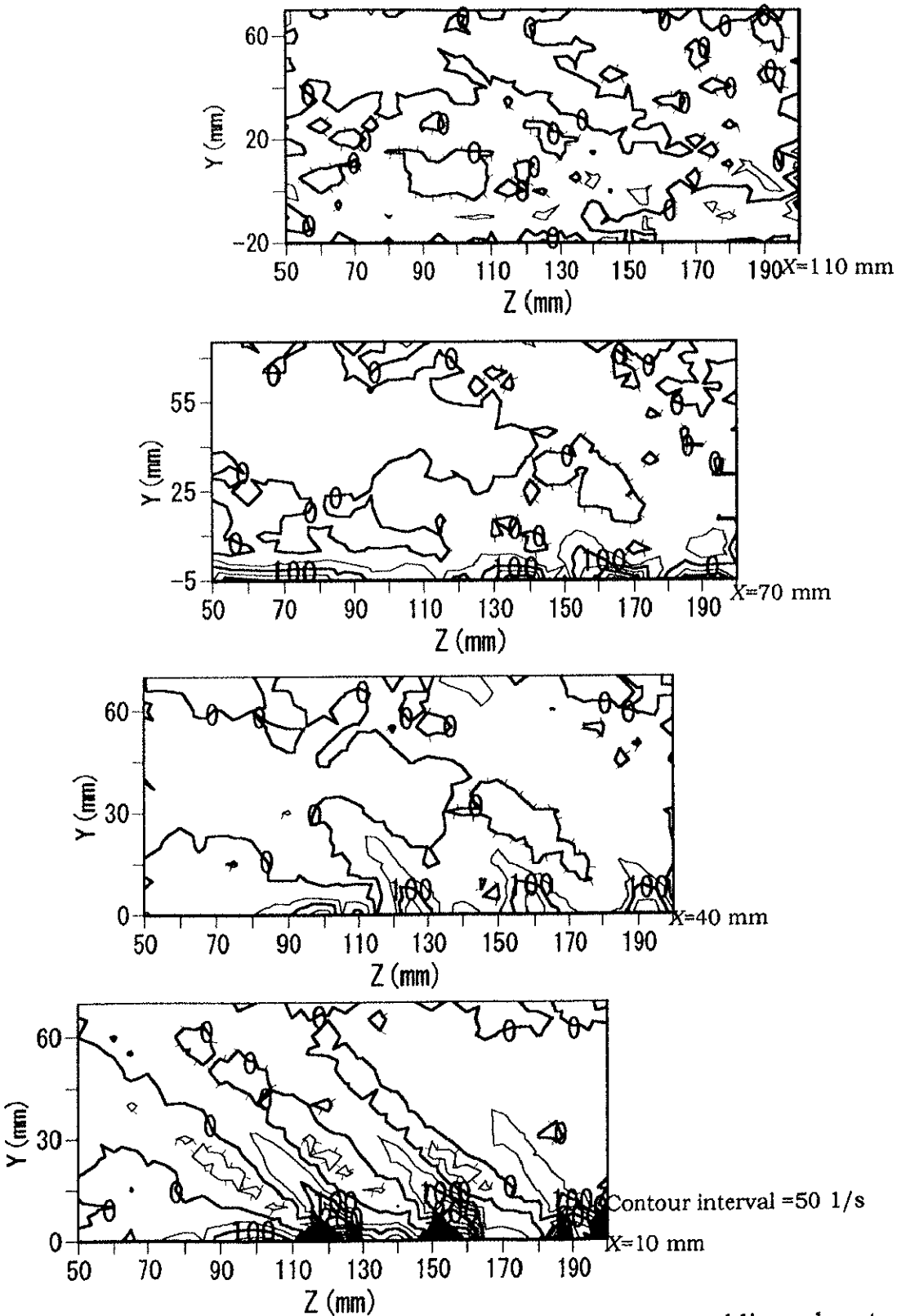

Figure 5.9 Contours of streamwise vorticity. Decorated lines denote negative vorticity (U_0=6.5 m/s, VR=5.6, f_p=20 Hz, α=20 deg).

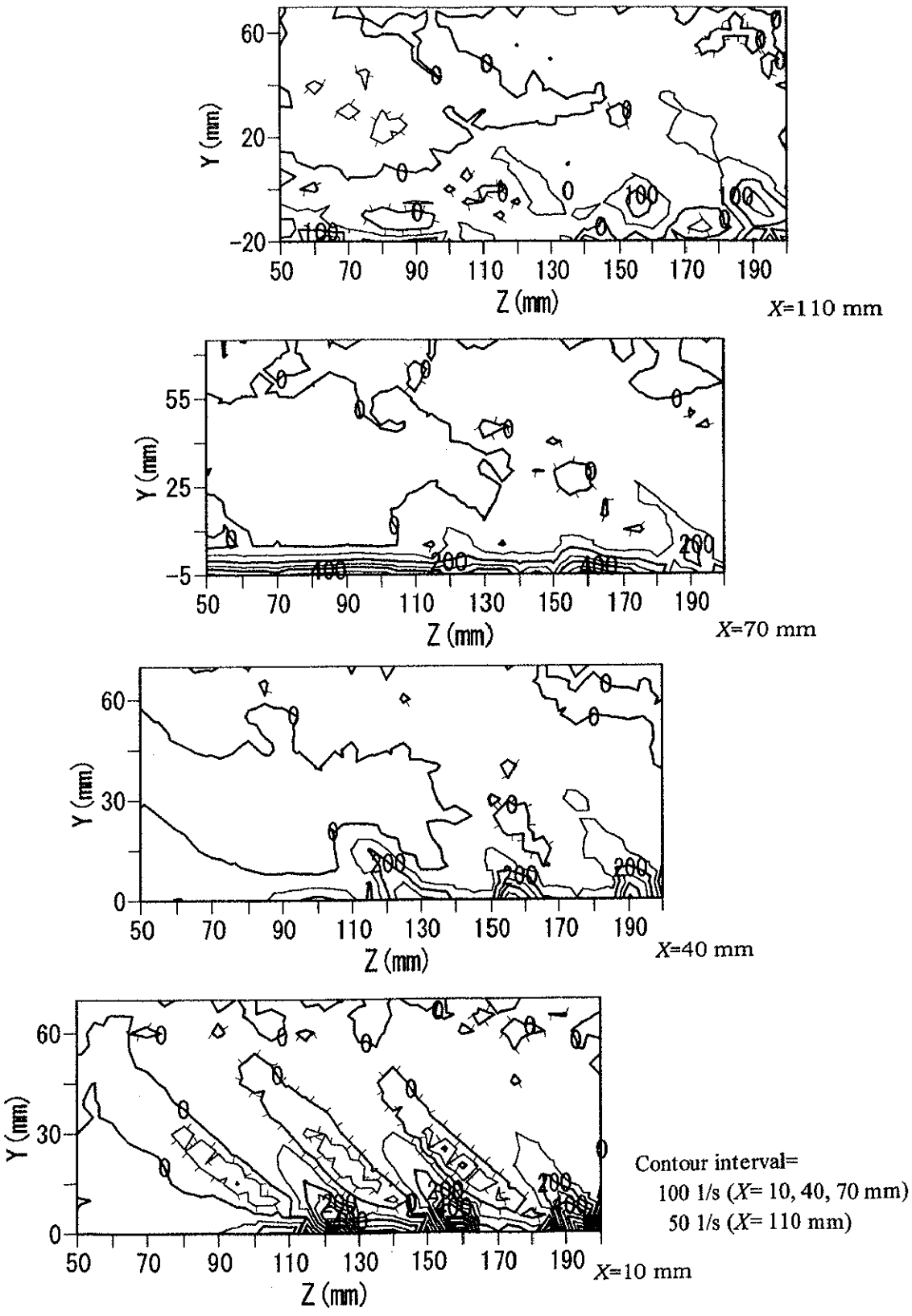

Figure 5.10 Contours of streamwise vorticity. Decorated lines denote negative vorticity (U_0=11.1 m/s, VR=5.6, f_p=20 Hz, α=20 deg).

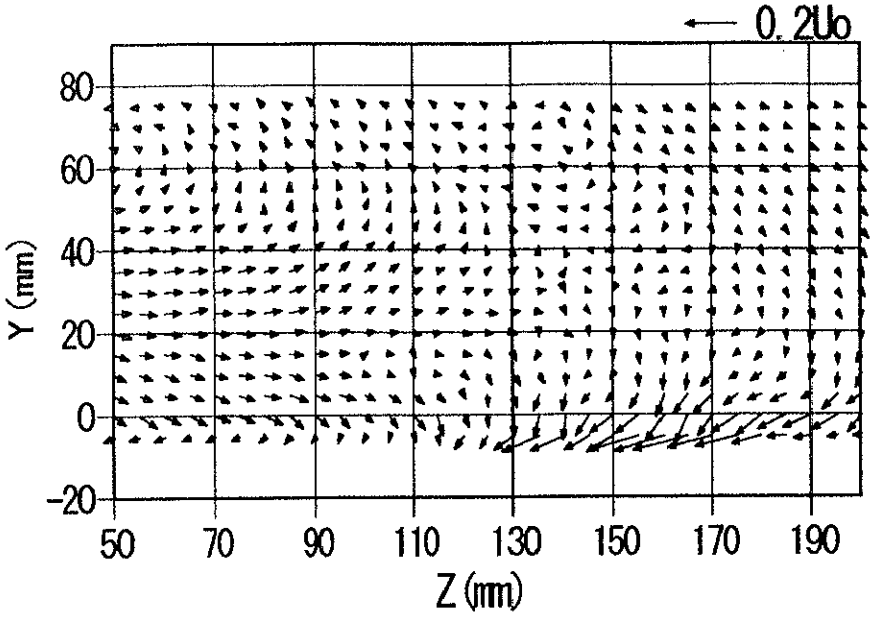

(a) X=70 mm

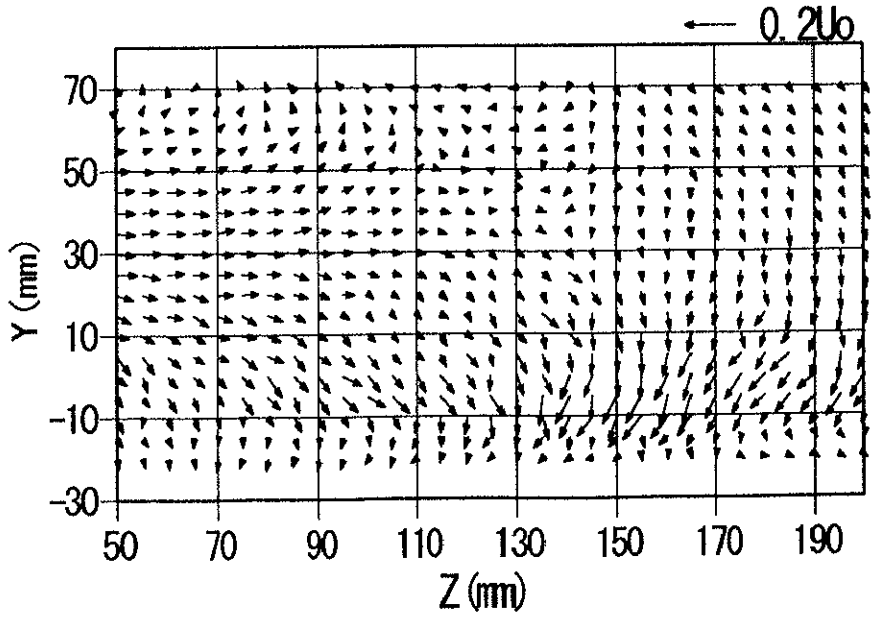

(b) X=110 mm

Figure 5.11 Secondary flow vectors (U_0=6.5 m/s, VR=5.6, f_p=20 Hz, α =20 deg).

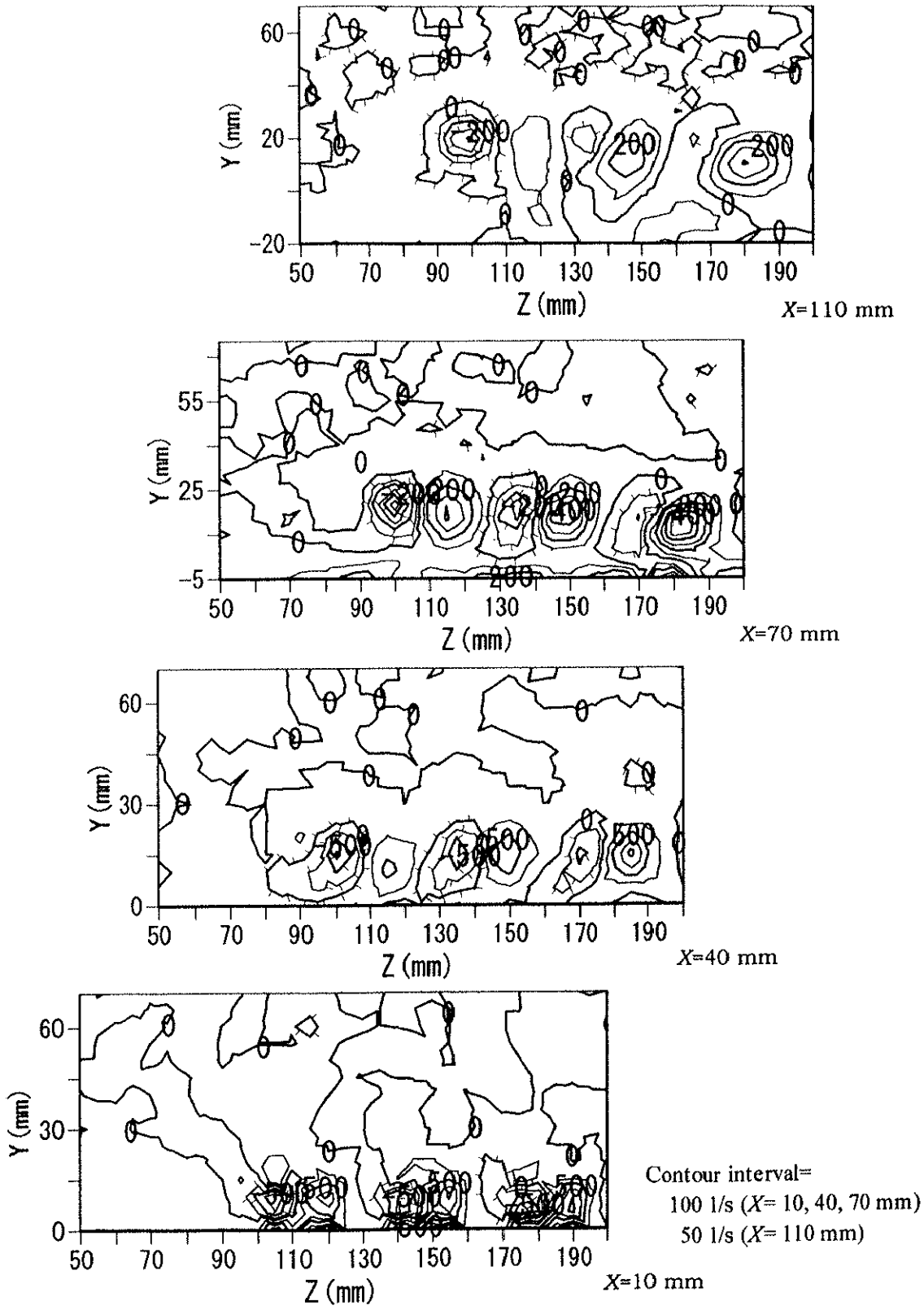

Figure 5.12 Contours of streamwise vorticity. Decorated lines denote negative vorticity (U_0=6.5 m/s, VR=9.5, α=20 deg).

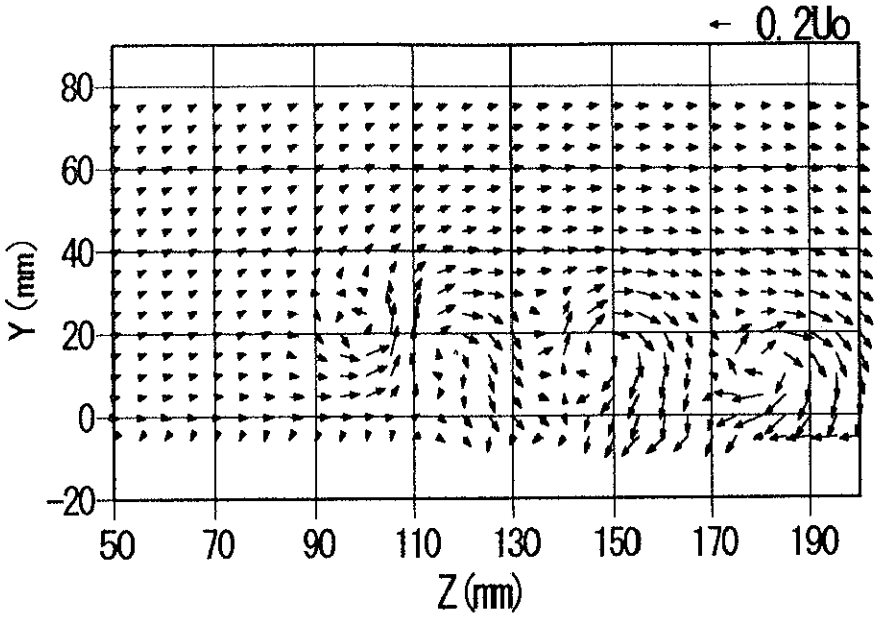

(a) X=70 mm

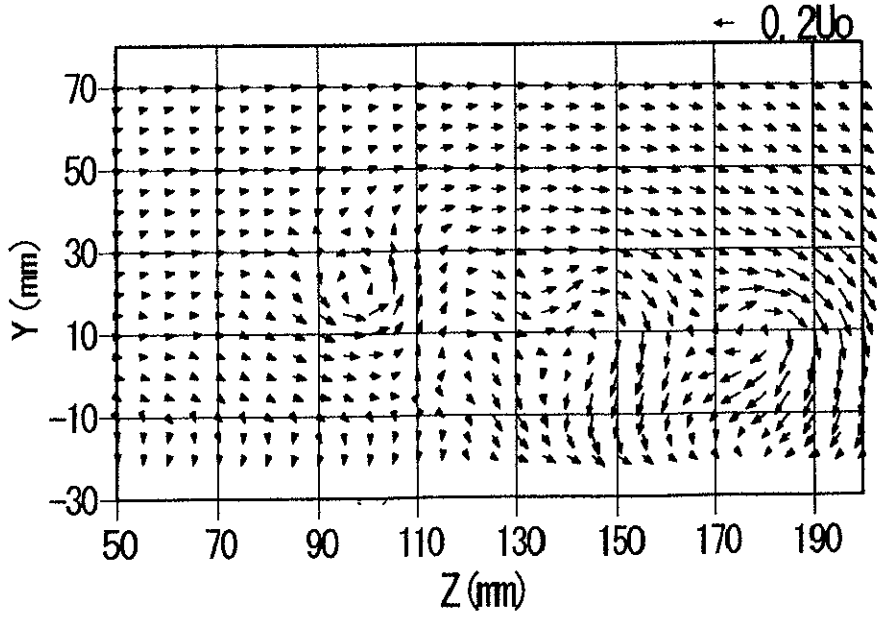

(b) X=110 mm

Figure 5.13 Secondary flow vectors (U_0=6.5, VR=9.5, α =20 deg).

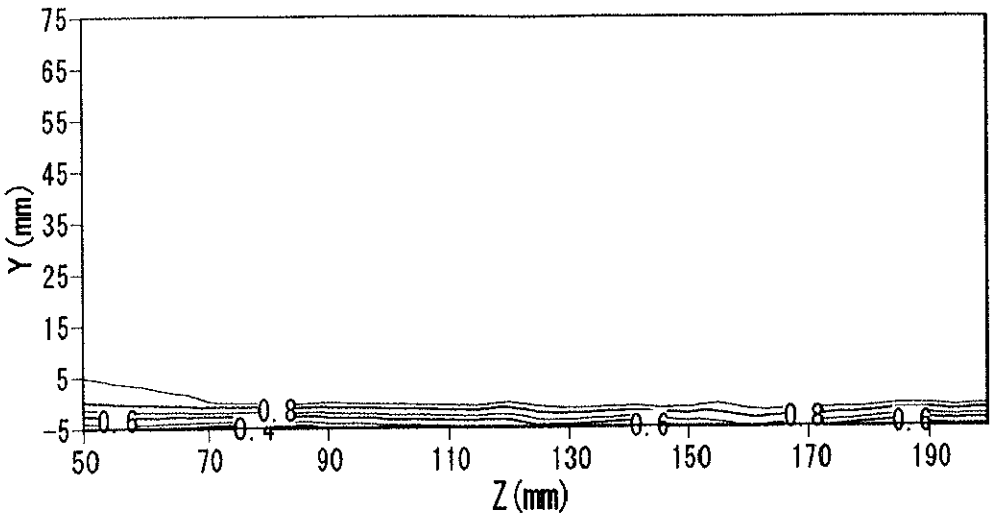

(a) Pulsed jets (VR=5.6, f_p=20 Hz)

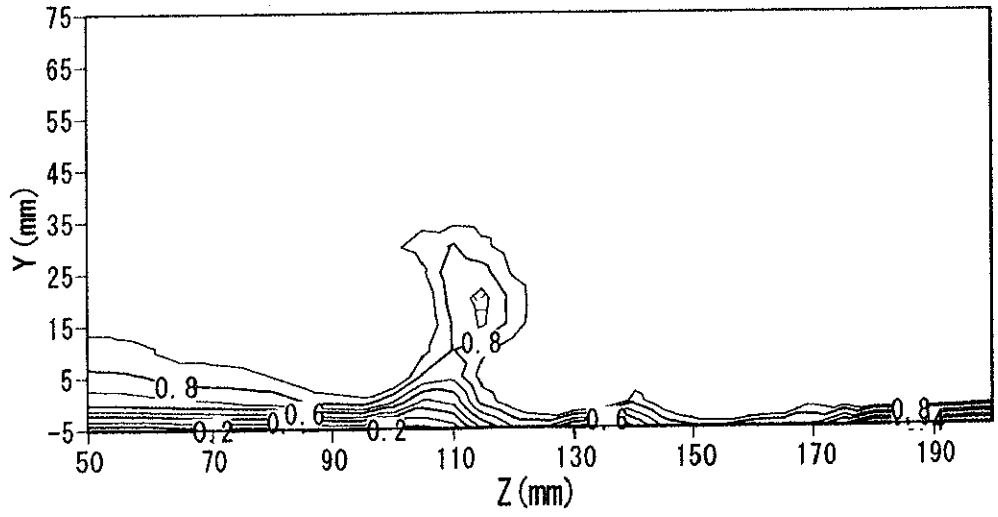

(b) Steady jets (VR=9.5)

Figure 5.14 U/U_0 contours at X=70 mm (U_0=6.5 m/s,α=20 deg). Contour interval=0.1.

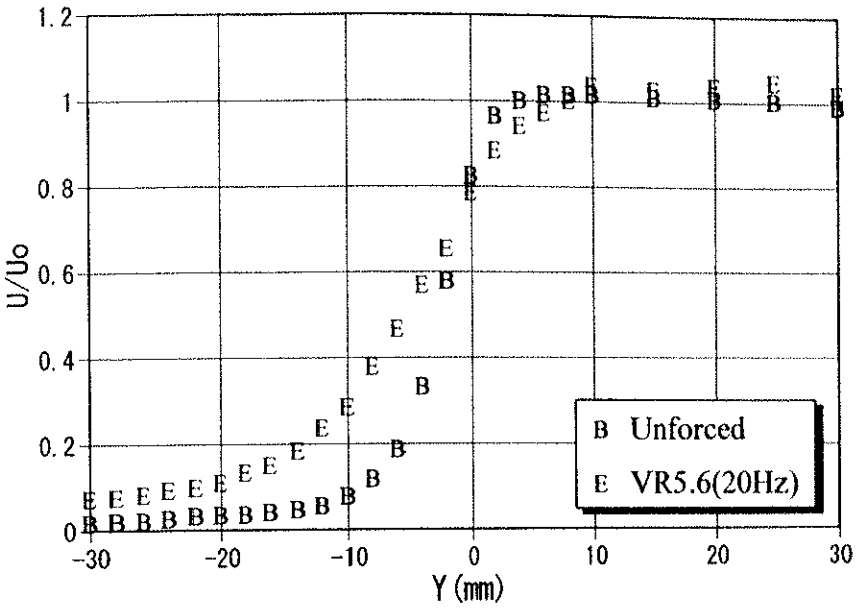

(a) U_0=6.5 m/s

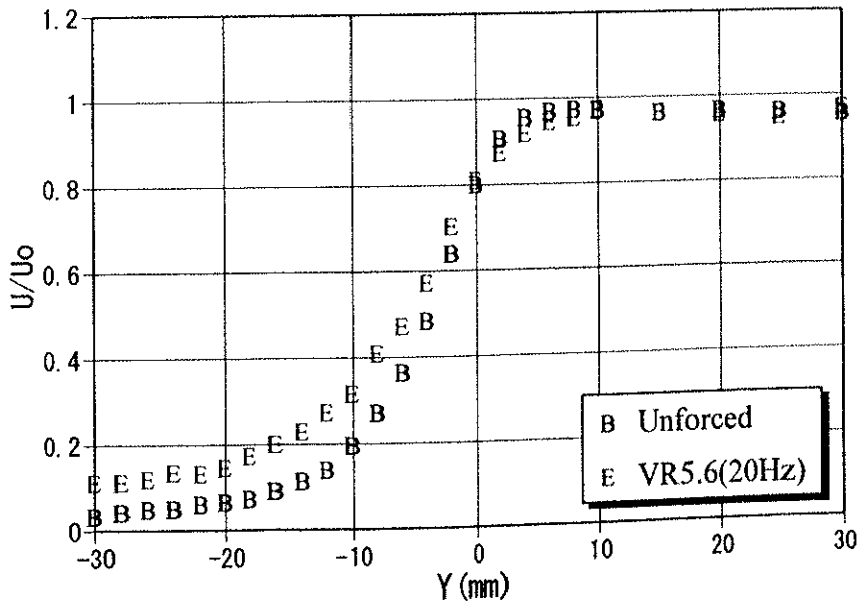

(b) U_0=11.1 m/s

Figure 5.15 Streamwise velocity profiles at X=110 mm (α=30 deg).

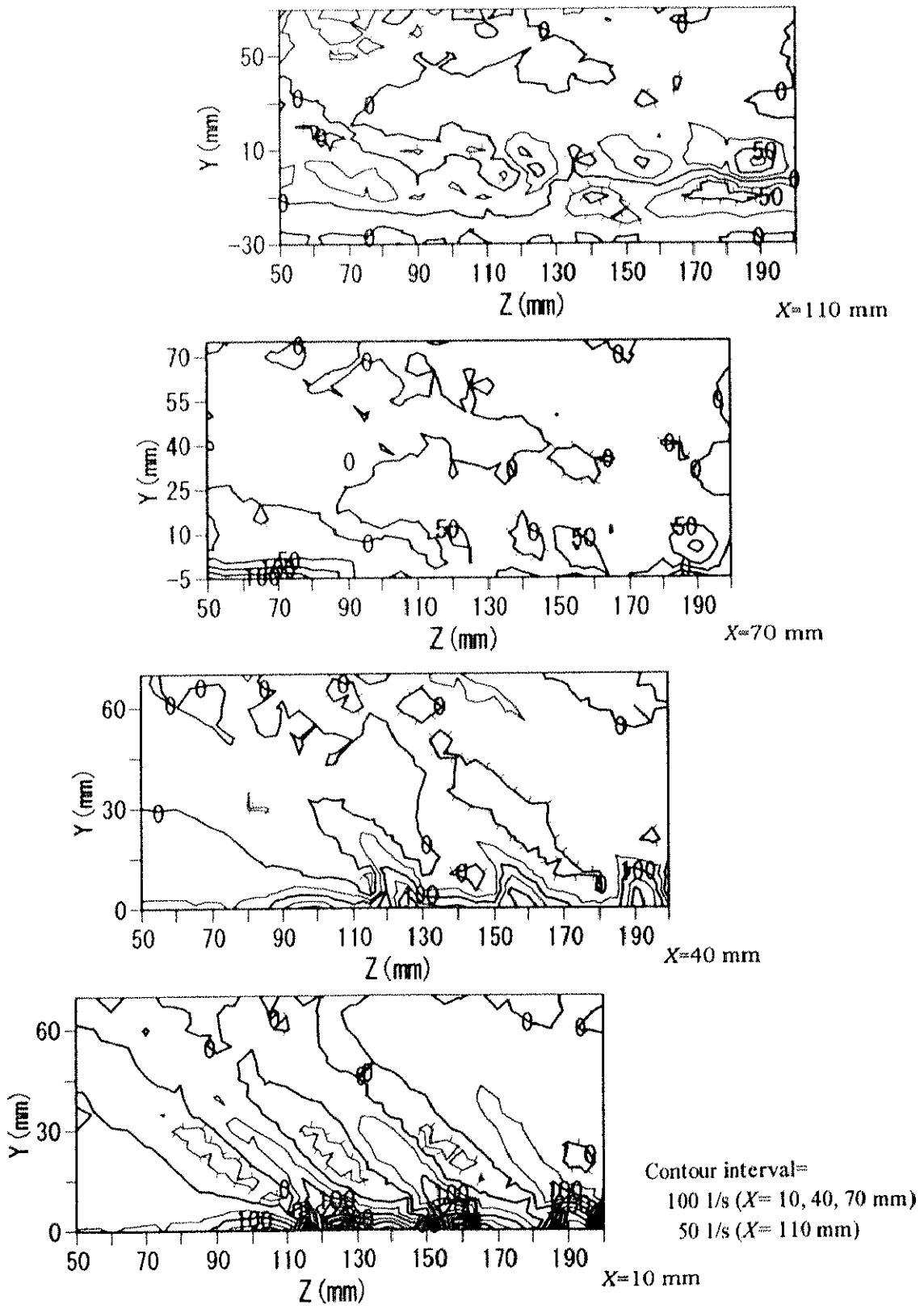

Figure 5.16 Contours of streamwise vorticity. Decorated lines denote negative vorticity (U_0=6.5 m/s, VR=5.6, f_p=20 Hz, α=30 deg).

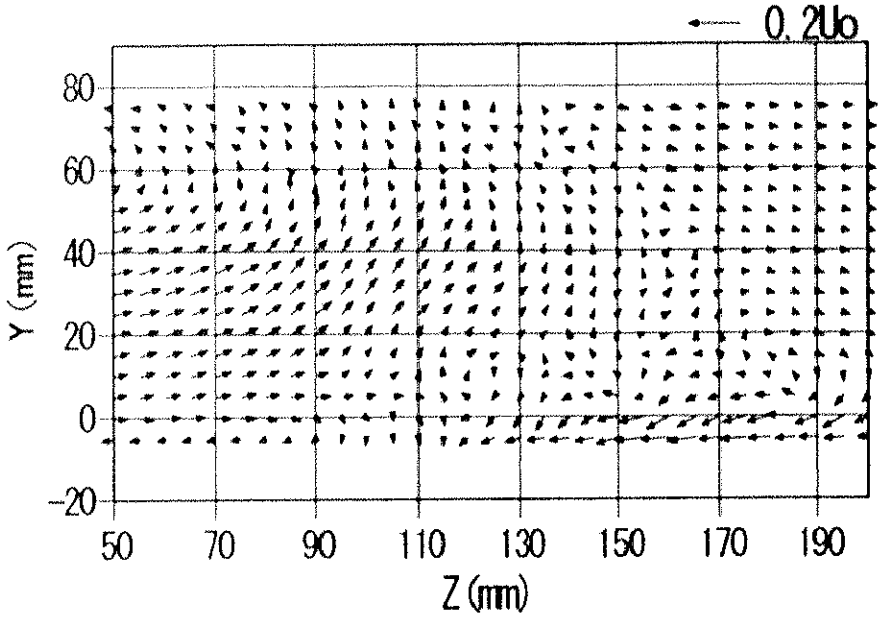

(a) X=70 mm

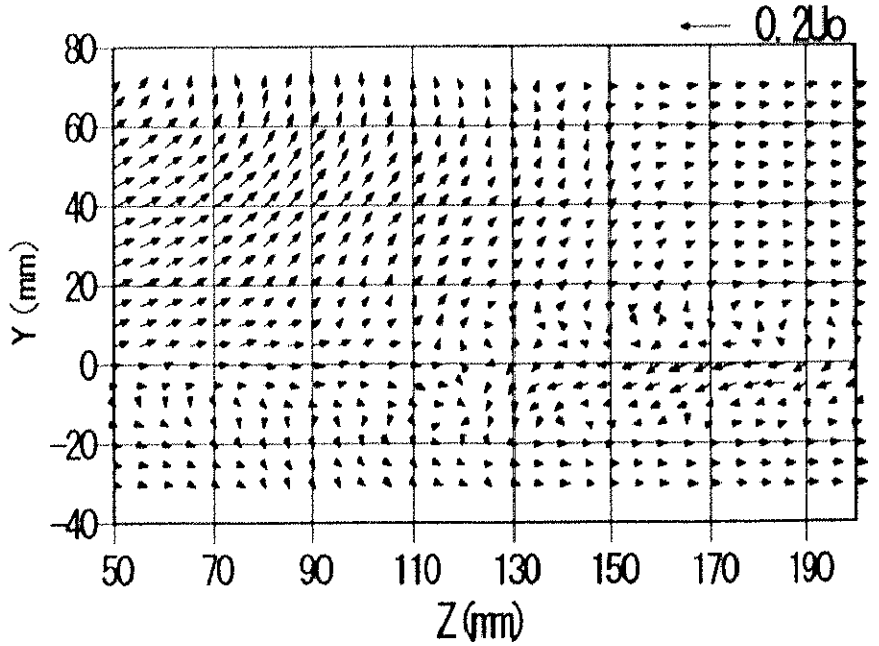

(b) X=110 mm

Figure 5.17 Secondary flow vectors (U_0=6.5 m/s, VR=5.6, f_p=20 Hz, α =30 deg).

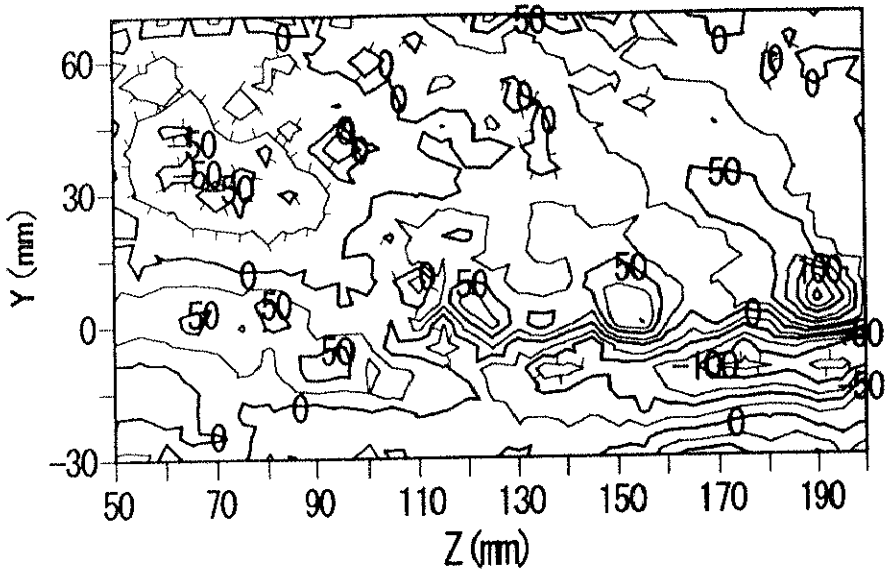

(a) Contours of streamwise vorticity (Decorated lines denote negative vorticity, Contour interval =25 1/s)

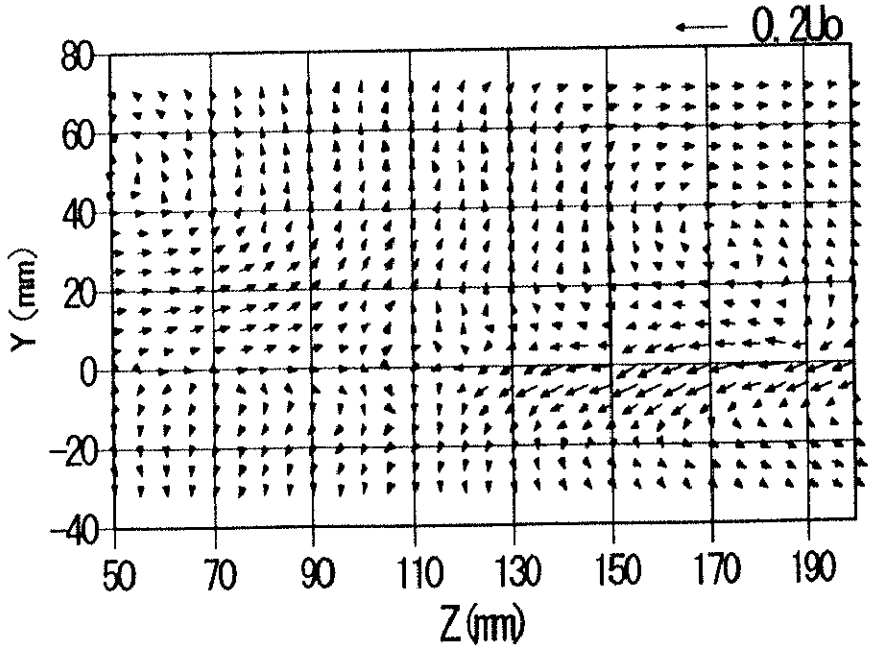

(b) Secondary flow vectors

Figure 5.18 Flow situation at X=110 mm (U_0=11.1 m/s, VR=5.6, f_p=20 Hz, α =30 deg).